

Journal of Engineering

journal homepage: www.jcoeng.edu.iq

Volume 31 Number 11 November 2025



Secrecy Rate in BD-RIS-Assisted Uplink Multi-User MIMO Systems Under Nakagami-m Fading with Passive Eavesdropping

Mina Fadhil Hasan 🎾 🕒 *, Aqiel Niama Almamori 🗘

Department of Electronics and Communications Engineering, College of Engineering, University of Baghdad, Baghdad, Iraq

ABSTRACT

With the evolution toward 6G wireless networks, ensuring secure communication has become increasingly important due to persistent risks of eavesdropping and unauthorized access. Beyond Diagonal Reconfigurable Intelligent Surfaces (BD-RIS) enhance control over wireless channels by independently manipulating both the phase and magnitude of reflected signals, thereby improving the physical-layer security of wireless communication systems. This paper investigates the performance of a BD-RIS-assisted uplink multi-user MIMO system operating under Nakagami-m fading conditions in the presence of a passive eavesdropper. Specifically, we analyze and compare the achievable sum rate and secrecy rate in scenarios both with and without a direct link between the users and the base station. Through detailed simulations, we demonstrate that BD-RIS achieves an improvement of 8.33% in secrecy rate than conventional diagonal RIS under comparable system parameters. Furthermore, we show that the amount of this enhancement is influenced by key system parameters, including the transmit power, the distance of the eavesdropper from the BD-RIS, and the density of active users within the network.

Keywords: BD-RIS, Secrecy rate, Multi-user MIMO, Nakagami-m fading, Physical layer security (PLS), 6G networks.

1. INTRODUCTION

Ensuring the secrecy and security of information transmission is a critical priority in modern wireless networks. With the fact that the Internet of Things (IoT) devices are increasing and the networks are evolving toward 6G, the risk of eavesdropping and confidential data breaches becomes more concerning. The inherent broadcast nature of wireless communication makes transmitted signals vulnerable to interception by unauthorized parties, raising significant challenges for maintaining information confidentiality and integrity (Mohammed, 2020). This necessitates innovative physical layer security solutions that can protect confidential information while maintaining communication efficiency.

*Corresponding author

 $Peer\ review\ under\ the\ responsibility\ of\ University\ of\ Baghdad.$

https://doi.org/10.31026/j.eng.2025.11.05

This is an open access article under the CC BY 4 license (http://creativecommons.org/licenses/by/4.0/).

Article received: 24/04/2025 Article revised: 20/07/2025 Article accepted: 30/09/2025 Article published: 01/11/2025



Reconfigurable Intelligent Surfaces (RIS) have emerged as a promising technology to address these challenges. A RIS is a two-dimensional array consisting of numerous low-cost, programmable elements capable of dynamically altering the phase of incident signals (Ji et al., 2021; Yang et al., 2023; Gao et al., 2024b). This capability enables unprecedented control over the wireless propagation environment, allowing signals to be directed toward intended receivers while being suppressed in the direction of potential eavesdroppers (Basar et al., 2019; Hamza et al., 2024).

Conventional RIS technology (also known as Diagonal RIS or D-RIS) primarily manipulates the phase of incident signals through a diagonal scattering matrix (Li et al., 2023a; Nerini et al., 2024, Almamori and Abbas, 2023). While effective, this approach limits the degrees of freedom available for channel optimization. Building upon this foundation, a more generalized form, Beyond Diagonal RIS (BD-RIS), has been developed to further enhance reconfigurability and security by manipulating both the phase and magnitude of incident signals through a full scattering matrix (Fang and Mao, 2024; Nerini et al., 2024; Santamaria et al., 2024).

In this work, the BD-RIS-assisted uplink multi-user MIMO system illustrated in **Fig. 1** is considered. Which includes the following: a multi-antenna base station (BS), K single-antenna users, BD-RIS, and a passive eavesdropper (EVE). Assuming that the information being exchanged between the users and the BS are transmitted using both direct and reflected (BD-RIS-assisted) links. The BD-RIS adjusts both the phase and magnitude of reflected signals in order to get maximum signal quality at the BS while trying to suppress it for the EVE. This figure provides a high level overview of the whole system components and communication paths. **(Khoshafa et al., 2024)** offers a review on the integration of RIS with physical layer security (PLS) in both the RF and the optical communication systems, considers a range of setups including multi antenna, mmWave, THz, UAV, D2D, and IoT networks. It also surveys optimization and machine learning techniques, performance analysis, and key challenges for RIS assisted PLS.

Also, multiple studies have focused on addressing the challenging problem of channel estimation in RIS-aided systems. (Zhou et al., 2024) proposed new CSI estimation frameworks using unstructured and geometric channel models for monostatic and bistatic full-duplex base stations, leveraging Khatri-Rao factorization and sparse multipath estimation to enhance accuracy while balancing complexity and pilot overhead. For mmWave communications, (Chen et al., 2023) introduced a novel channel estimation protocol using compressive sensing to estimate cascaded channels in RIS-aided multi-user MIMO systems. Their approach develops a sparse representation based on two-dimensional sparsity structure and employs a two-step joint estimation procedure with promising simulation results. (Demir and Björnson, 2022) approached channel estimation from a different angle, considering spatial correlation and random phase shifts. They proposed Bayesian estimators, low-complexity phase-shift selection techniques, and a fixed-point algorithm for power control to enhance spectral efficiency.

Research has also explored novel RIS architectures to expand functionality. (Liu et al., 2021) presented a Simultaneously Transmitting and Reflecting RIS (STAR-RIS) design, highlighting key differences from conventional RIS and proposing three operational protocols: energy splitting, mode switching, and time switching for next-generation networks. Building on this concept, (Wu et al., 2022) proposed efficient channel estimation schemes for STAR-RIS-assisted systems using Time Switching (TS) and Energy Splitting (ES) protocols. (Al-Nahhas et al., 2021) examined the performance of RIS-aided Cell-Free



massive MIMO systems in multi-user downlink scenarios, deriving closed-form achievable rate expressions under imperfect CSI and demonstrating the potential of RIS deployment for enhanced coverage and throughput.

Several recent studies have focused specifically on BD-RIS technology. (Santamaria et al., 2024) optimized the achievable rate of a MIMO link by jointly optimizing the transmit covariance matrix and BD-RIS parameters. Using Takagi decomposition and an algorithm on the unitary manifold, they demonstrated improved rates compared to diagonal RIS, particularly with increased streams, BD-RIS elements, or transmission power. For multisector applications, (Samy et al., 2025) investigated a BD-RIS-aided system with Time Switching protocol, analyzing sector configuration trade-offs and deriving exact closed-form outage probability and Symbol Error Probability expressions for Rician fading channels. (Li et al., 2024c) proposed methods for multi-antenna and multi-user systems with BD-RIS in different operational modes, developing beamforming algorithms and analyzing the trade-off between estimation overhead and transmission performance. Similarly, (Yahya et al., 2024) designed a two-stage BD-RIS optimization approach for the scattering matrix and base station precoding, demonstrating enhanced interference nulling capabilities.

In the security domain, (Singh et al., 2024) investigated active RIS in multi-user uplink NOMA systems, maximizing sum secrecy rate in the presence of an eavesdropper. Their Alternating Optimization (AO) based algorithm showed superior secrecy performance compared to passive RIS and Space Division Multiple Access (SDMA) approaches. (Hamza et al., 2024) analyzed secrecy rate and secrecy outage probability in an RIS-enhanced uplink NOMA system under Nakagami-m fading. For BD-RIS specifically, (Nerini et al., 2024) proposed a low-complexity closed-form global optimal solution for scattering matrix design in reflective and transmissive modes, achieving performance upper bounds for various channel realizations. Additional contributions include (Mishra et al., 2024), who proposed a base station-side BD-RIS deployment in massive MIMO systems, optimizing BD-RIS coefficients via a manifold algorithm and statistical CSI, while (Fang and Mao, 2024) developed a closed-form solution for BD-RIS passive beamforming to maximize effective channel gains.

Following the most recent literature, our analysis assumes a passive nature regarding both RIS and BD-RIS, because of their low power consumption, low cost, and also because their reflecting elements don't have any active RF components. Although active RIS gives an additional signal amplification, this comes at the expense of higher system complexity and noise, making this passive architecture assumption more appropriate for secure and large-scale deployments (Li et al., 2024c).

Despite these advances, the comparative performance analysis of BD-RIS versus conventional D-RIS for secure communications under realistic fading conditions remains insufficiently explored, particularly in multi-user MIMO uplink scenarios with eavesdroppers. Most existing works either focus on single-user settings, downlink transmission, or simplified channel models that may not capture the complexity of real-world wireless environments. In this paper, we address this gap by investigating the performance of a BD-RIS-assisted uplink multi-user MIMO system under Nakagami-m fading channels, considering the presence of an eavesdropper attempting to intercept the transmitted information. Our key contributions include:

1. A comprehensive system model for BD-RIS-aided secure uplink transmission in multi-user MIMO networks under Nakagami-m fading.



- 2. Development of an alternating optimization framework to jointly optimize the transmit covariance matrix and the BD-RIS scattering matrix for sum rate maximization, tailored for a multi-user uplink system with single-antenna users and a MIMO base station under Nakagami-m fading.
- 3. Comparative analysis of sum rate and secrecy rate for two practical scenarios:
 - When the direct link between the base station and users is fully blocked by an obstacle.
 - When the direct link is present alongside the BD-RIS-assisted path.
- 4. Quantification of secrecy rate enhancement offered by BD-RIS compared to conventional D-RIS across various system parameters.
- 5. Analysis of how power transmits, eavesdrop distance, and user density influence the security performance gains of BD-RIS.

2. SYSTEM MODEL

Consider the system in **Fig. 1**, which consists of a multiple-input multiple-output (MIMO) base station (BS) equipped with M active antennas, Beyond-Diagonal Reconfigurable Intelligent Surfaces (BD-RIS) with N passive antennas, K legitimate users, and an eavesdropper (EVE). Assuming uplink communication between the users and the BS, with two scenarios to be analyzed: the first is when the direct channel is available with the aid of BD-RIS, while the second is when an obstacle fully blocks the direct link, and the communication relies only on the path via BD-RIS.

The system also includes a passive eavesdropper attempting to listen to this communication and get the information being communicated between legitimate parties. Each legitimate user, as well as the eavesdropper, is equipped with a single antenna. Also, assume that the entire system operates in time-division duplexing (TDD) mode where the uplink and downlink channels are reciprocal (Laas et al., 2020; Tang et al., 2021). EVE assumed to change position away from the BD-RIS. Also, the between elements' spacings of the passive BD-RIS is more than or equal to half the wavelength at the frequency of operation so that there is no mutual coupling between the elements. (Li et al., 2024b; Mishra et al., 2024)

2.1 Channel and Signal Model

Let the channels between the BS and i_{th} user, the BS and BD-RIS, BD-RIS and the i_{th} user, passive eavesdropper (EVE) and the i_{th} user ,and between BD-RIS and EVE to be: $\mathbf{h_i} \in \mathbb{C}^{M \times 1}$, $\mathbf{F} \in \mathbb{C}^{M \times N}$, $\mathbf{g_i} \in \mathbb{C}^{N \times 1}$, $v_i \in \mathbb{C}^{1 \times 1}$, $\mathbf{e} \in \mathbb{C}^{N \times 1}$, respectively. The phase shift matrix of the passive BD-RIS denoted as $\Phi \in \mathbb{C}^{N \times N}$ satisfies the unitary and symmetry constrains, Eq. (1) and Eq. (2) (Fang and Mao, 2024; Li et al., 2024a).

$$\Phi = \Phi^T \tag{1}$$

$$\Phi^{H} * \Phi = I \tag{2}$$

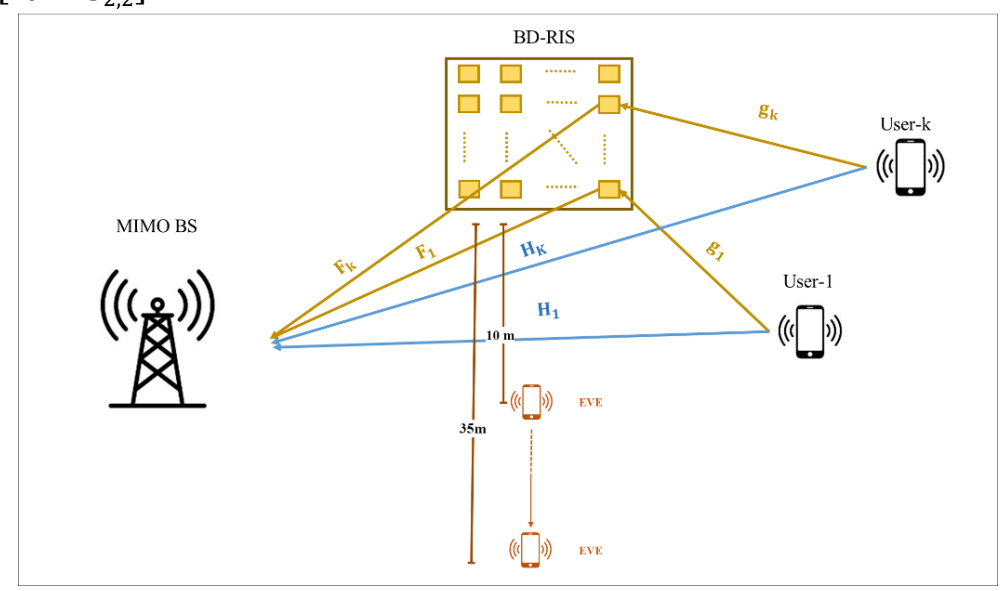
Where (.)^T refers to transpose and (.)^H refers to Hermitian. Besides being unitary and symmetric, the scattering matrix is non-diagonal in BD-RIS unlike that of RIS, as can be seen in Eq. (3) and Eq. (4) which illustrate a simplified 2-port example for BD-RIS and RIS respectively. This difference arises from the BD-RIS architecture in which each antenna element is connected to every other element(Li et al., 2023b), which in return differs from the single connected RIS as illustrated in Fig. 2, which shows the connections in RIS and BD-RIS assuming 4-antenna elements in both.



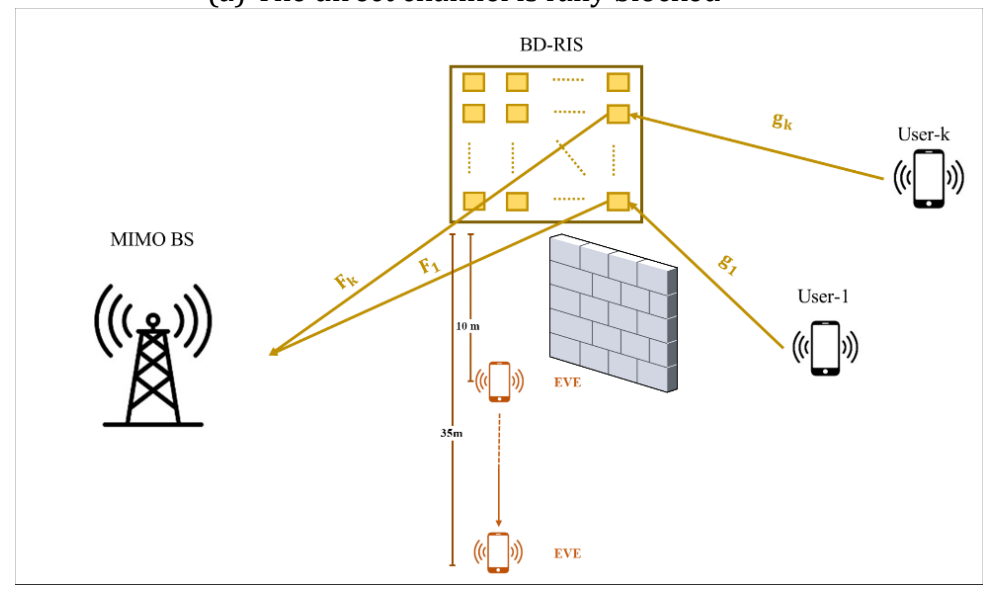
$$\Phi_{BD-RIS} = \begin{bmatrix} S_{1,1} & S_{1,2} \\ S_{2,1} & S_{2,2} \end{bmatrix}$$

$$\Phi_{RIS} = \begin{bmatrix} S_{1,1} & 0 \\ 0 & S_{2,2} \end{bmatrix}$$
(3)

$$\Phi_{RIS} = \begin{bmatrix} S_{1,1} & 0\\ 0 & S_{2,2} \end{bmatrix} \tag{4}$$



(a) The direct channel is fully blocked



(b) The direct link is present.

Figure 1. The proposed system model

The propagation model consists of large-scale and small-scale fading effects for all channels. The large-scale fading follows a distance-dependent path loss model given by (Khaled et al., 2022):

$$L\left(d_{z}\right) = d_{z}^{-\alpha} \tag{5}$$

where d_z represents the distance between the transmitter and receiver, and α is the path loss exponent.



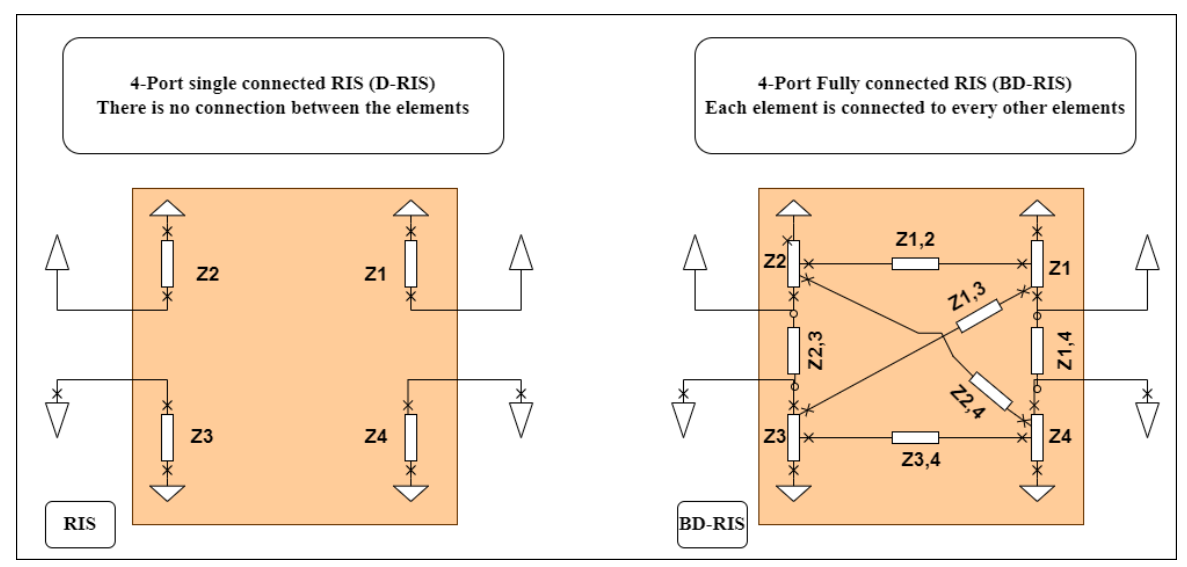


Figure 2. RIS versus BDRIS architecture (Shen et al., 2022)

In our work, Nakagami-m is utilized as a small scale fading distribution type across all wireless links. This model is selected because of its ability to accurately capture a wide range of wireless channels by varying the shape parameter m. In particular, Nakagami-m fading can model Rayleigh fading when setting (m=1), approach Rician fading for any moderate values of m, and approximate the free space nonfading channels when $m\to\infty$. As such, it is widely known for evaluating the secrecy performance of wireless systems under diverse propagation environments. The probability density function (PDF) of this distribution is expressed as (Gómez-Déniz and Gómez-Déniz, 2024):

$$q(y;m) = \frac{m^m y^{m-1}}{\Gamma(m)} e^{-my}, \forall y > 0$$
 (6)

Where m is the Nakagami fading parameter. The gamma function $\Gamma(u)$ is as follows **(Hamza et al., 2024)**:

$$\Gamma\left(u\right) = \int_0^\infty v^{u-1} e^{-v} dv \tag{7}$$

After channel estimation (e.g., using an LS channel estimator) (Ding, 2023; Abdul Majed and Omran, 2020), the K users transmit their information to the intended party, which in this case is the BS. Accordingly, the received signals at the BS and the eavesdropper (EVE) are given by (Hamza et al., 2024):

$$y_{BS-i} = \sum_{i=1}^{k} \sqrt{S_i} (h_i + F \oplus g_i) x_i' + n_i$$
 (8)

$$\mathbf{y}_{EVE-i} = \sum_{i=1}^{k} \sqrt{S_i} \left(v_i + \mathbf{e}' \, \Phi \, \mathbf{g}_i \right) \mathbf{x}_i' + \mathbf{n}_i \tag{9}$$

Where S_i is the power transmitted from the i_{th} user, the additive white Gaussian noise (AWGN) is represented as $\mathbf{n_i} \sim \mathcal{CN}$ $(0, \sigma^2 \mathbf{I})$, and the information being sent from the i_{th} user during the uplink transmission time period $(\tau_{up-data})$ (Mohammed and Almamori, 2024) is $\mathbf{x_i} \in \mathbb{C}^{\tau_{up-data} \times 1}$.



Fig. 3 presents a flowchart to clarify the main steps, including parameter initialization, pilot transmission, channel estimation, joint optimization, and data transmission.

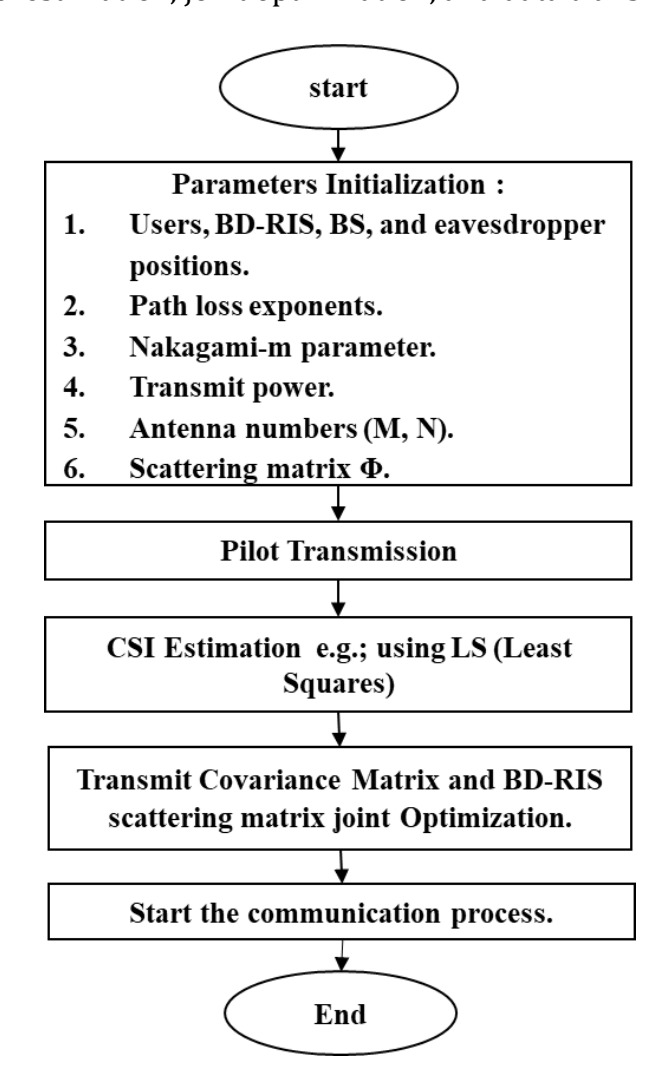


Figure 3. Flowchart for the proposed BD-RIS-assisted uplink communication process.

2.2 Scattering Matrix Optimization

In order to maximize the sum rate at the BS side, the scattering matrix of the BD-RIS has to be optimized. In BD-RIS assisted systems, the scattering matrix controls how the incident signals are reflected and combined at the receiver side, which, as a result, controls the received signal quality at the BS and the interference that EVE experiences. Without the utilization of any optimization technique, the degrees of freedom provided by the BD-RIS cannot be fully exploited, which, as a result, leads to suboptimal signal enhancement and limited secrecy performance. Using an optimization technique allows for constructive combining at the BS, improving both the spatial selectivity and the suppression of signal leakage towards unintended receivers. This is critical in multi-user MIMO scenarios with complex fading settings that may lead to severe inter-user interference (IUI) and reduced overall network efficiency. While we adopt the optimization framework presented in (Santamaria et al., 2024). Our work differs by incorporating multi-users, each having a single antenna, with a MIMO BS.



Besides, we consider a more general Nakagami-m channel model. Which is unlike the work in (Santamaria et al., 2024), that considers point-to-point (P2P) MIMO transmission where a single transmitter with N_T antennas communicates with a single receiver with N_R antennas, with $N_T = N_R$, focusing on data streams. The algorithm mainly involves optimizing the transmit covariance matrix \mathbf{R}_{xx} from the users to the BS for fixed Φ followed by optimizing the scattering matrix Φ for fixed \mathbf{R}_{xx} . This process is repeated iteratively until convergence is achieved.

According to Eq. (8) and Eq. (9), the total channels from the users to the BS and EVE are:

$$H_{eq-BS} = H + F \Phi G \tag{10}$$

$$\boldsymbol{h}_{\boldsymbol{e}\boldsymbol{q}-\boldsymbol{E}\boldsymbol{V}\boldsymbol{E}} = \boldsymbol{v} + \boldsymbol{e}' \,\Phi \,\boldsymbol{G} \tag{11}$$

Where $\mathbf{H}_{\mathbf{eq}-\mathbf{BS}} \in \mathbb{C}^{M \times K}$ and $\mathbf{h}_{\mathbf{eq}-\mathbf{EVE}} \in \mathbb{C}^{1 \times K}$.

The optimized covariance matrix from the users to the BS $\mathbf{R}_{xx} \in \mathbb{C}^{K \times K}$ is:

$$R_{xx} = V S V^H \tag{12}$$

Where $\mathbf{V} \in \mathbb{C}^{K \times K}$ is the left eigenspace of the equivalent channel matrix \mathbf{H}_{eq-BS} and $\mathbf{S} \in$ $\mathbb{C}^{K \times K}$ is a diagonal matrix representing the optimal power allocated given by the waterfilling method, in which it satisfies the power constraint $\sum_i S_i = S$, where S_i represents the power allocated for the ith user.

After optimizing $\mathbf{R}_{\mathbf{x}\mathbf{x}}$ for fixed Φ , the equivalent channel in Eq. (10) becomes (Santamaria et al., 2024):

$$H_{eq-BS-new} = (H + F \oplus G) * V * S^{1/2}$$
 (13)

2.3 SINR and Sum Rate

After optimizing both R_{xx} and Φ , the SINR at both the base station (BS) and the eavesdropper (EVE) is computed using the following expressions:

$$\gamma_{BS} = \frac{1}{\sigma^2} \left(H_{eq-BS-new} * H_{eq-BS-new}^H \right)$$

$$\gamma_{EVE} = \frac{1}{\sigma^2} \left(h_{eq-EVE} * h_{eq-EVE}^H \right)$$
(14)

$$\gamma_{EVE} = \frac{1}{\sigma^2} \left(\mathbf{h}_{eq-EVE} * \mathbf{h}_{eq-EVE}^H \right) \tag{15}$$

The sum rate at both the base station (BS) and the eavesdropper (EVE) (Karim et al., 2023; **Zhang et al., 2023)** is then determined using the following expressions:

$$R_{BS} = log_2(det(I_M + \gamma_{BS}))$$
 (16)

$$R_{EVE} = log_2(1 + \gamma_{EVE}) \tag{17}$$

2.4 Secrecy Rate

When an eavesdropper is present in the network, attempting to intercept confidential information being transmitted from the legitimate users to the base station (BS), the secrecy rate is calculated as follows (Gao et al., 2024a; Hamza et al., 2024):

 $(RiceFactor+1)^2$



$$S_R = [R_{BS} - R_{EVE}]^+ = [log_2(det (I_M + \gamma_{BS})) - log_2(1 + \gamma_{EVE})]^+$$
 (18)

Where $[A]^+ \triangleq max(0, A)$.

Nakagami-m parameter

3. RESULTS AND DISCUSSION

MATLAB R2023b (MathWorks, released in September 2023) is used to simulate the wireless network depicted in **Fig. 1**, where the base station (BS) and the BD-RIS are positioned at coordinates (0,0,20) and (50,5,5), respectively. The distances between the K users and the BD-RIS follow a sequential pattern of (5,15,25) meters, while the eavesdropper is assumed to move away from the BD-RIS, starting from 10 to 35 meters. The BS is equipped with (M = 64) active antennas, which is a typical configuration in MIMO research, providing a balance between computational complexity and simulation feasibility **(Chen et al., 2023)**, whereas the BD-RIS consists of (N = 128) passive reflecting elements. The total transmission power varies from 30 dBm to 40 dBm. Regarding large-scale fading parameters, the path loss at a reference distance of (d = 1) meter is set to -28 dB, with path loss exponents of 3.75 for direct links and 2.0 for links through the BD-RIS. To ensure accuracy, Monte Carlo simulations are conducted. All the parameters used in the simulation is mentioned in **Table 1**.

Parameter Value BS coordinates (X, Y, Z) (0, 0, 20)BD-RIS coordinates (X, Y, Z) (50, 5, 5)The distance between 1st user and BD-RIS 5 m The step increment between 1st user and kth user with respect to 10 m BD-RIS (e.g., 2nd user is 15 m from the BS and so on) Eavesdropper distance from the BD-RIS (10: 35) m Number of BS antennas, M 64 Number of BD-RIS passive antennas, N 128 Power range, S total (30: 40) dBm Reference distance, do 1 m Reference path loss, L(do) -28 dB Path loss exponents of direct links, α 3.75 Path loss exponents of links through the BD-RIS, α 2 Number of Monte Carlo realizations realization

Table 1. Simulation Parameters

The main findings of our simulation are analyzed and discussed in this section. Specifically, **Figs. 4 and 5** illustrate that the secrecy rate increases with both transmit power and the eavesdropper's distance from the RIS. This is expected because higher power enhances the received signal strength at the BS, while increasing the separation between the eavesdropper and the BD-RIS weakens the ability of the eavesdropper to intercept the transmitted signals. Additionally, BD-RIS consistently outperforms D-RIS in all scenarios, whether the direct link is fully blocked **Fig. 4** or present **Fig. 5**. Besides, BD-RIS generates significant improvements in secrecy rate through minor adjustments to transmit power or eavesdropper's distance, whereas D-RIS needs substantial changes in both parameters to achieve similar results.



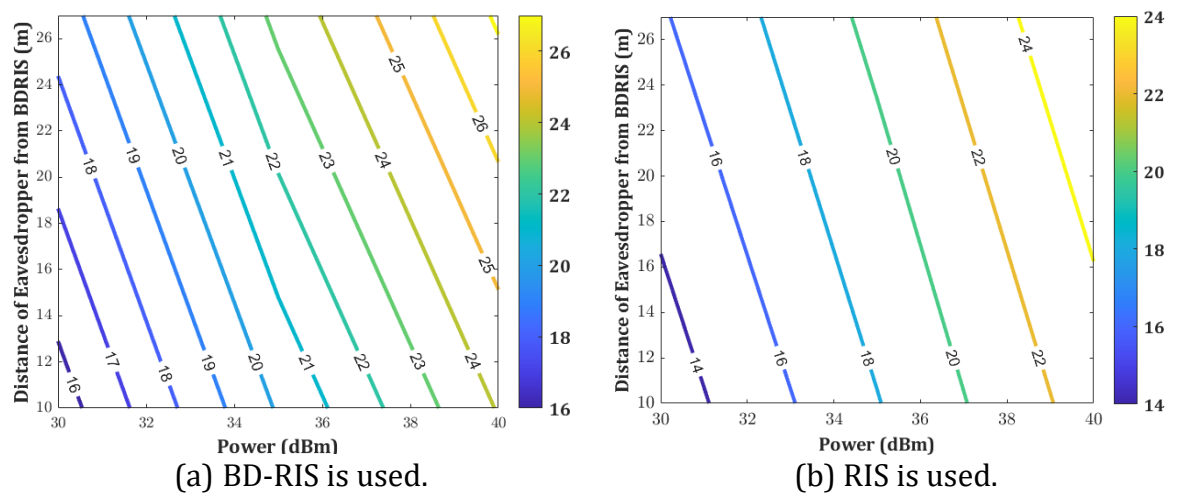


Figure 4. Secrecy rate comparison at the BS when BD-RIS and RIS are used in their respective channels, with the direct channel fully blocked by an obstacle.

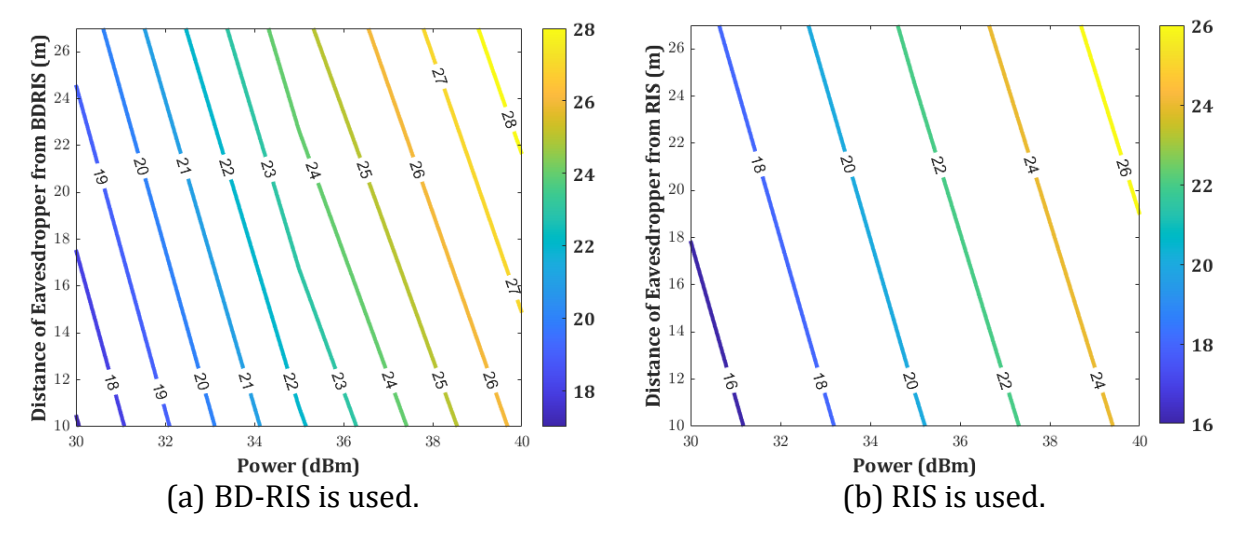


Figure 5. Secrecy rate comparison at the BS when BD-RIS and RIS are used in their respective channels, with the present of the direct channel.

This enhancement arises mainly from BD-RIS's non-diagonal scattering matrix Eq. (3), which allows it to jointly control both the magnitude and phase of the reflected signals, rather than phase only as it is the case in D-RIS. This additional degree of freedom enables BD-RIS to optimize signal power allocation and directional more effectively, enhancing the received signal strength at the BS while minimizing leakage toward the eavesdropper. In contrast, D-RIS, with its diagonal scattering matrix Eq. (4), is restricted to phase-only adjustments, limiting its capability to manipulate the wireless channel for secrecy enhancement. As a result, BD-RIS achieves an 8.33% improvement in secrecy rate compared to D-RIS, demonstrating its ability to dynamically shape the propagation environment, reinforce the BS's signals, and mitigate the eavesdropper's ability to receive them.

However, this improvement's percentage of BD-RIS over D-RIS is not constant and depends on several factors, particularly the number of users transmitting to the base station (BS). As shown in **Fig. 6**, BD-RIS maintains improved performance even as the number of users increases, whereas D-RIS experiences noticeable degradation. This arises because BD-RIS's non-diagonal scattering matrix enables more effective joint optimization of reflected signal



power and phase, mitigating inter-user interference while preserving strong signal enhancement at the BS. In contrast, D-RIS, with its phase-only control, lacks the ability to dynamically adjust power distribution, leading to suboptimal performance in multi-user scenarios. This limitation becomes more observable as user density increases.

Furthermore, **Fig. 7** reinforces our previous findings by demonstrating that the sum rate at the BS **Fig. 7** (a) is higher when utilizing BD-RIS, whereas the eavesdropper's sum rate **Fig. 7** (b) is higher when utilizing RIS; especially at high transmitted power. This further validates BD-RIS's ability to enhance the signal strength at the BS while effectively suppressing the eavesdropper's reception.

In addition, to further emphasize on BD-RIS's ability to create a smart environment regardless of the fading channel type to enhance the sum rate at the receiver, and hence the secrecy rate, **Fig. (8)** demonstrates its robust performance across Rayleigh, Rician, and freespace channels. This is achieved by adjusting the Nakagami-m parameter to $1, \frac{(RiceFactor+1)^2}{2*RiceFactor+1}$, and approximate to infinite. The results highlight BD-RIS's effectiveness in enhancing the secrecy rate across various fading environments, effectively making all channels perform comparably to free-space conditions.

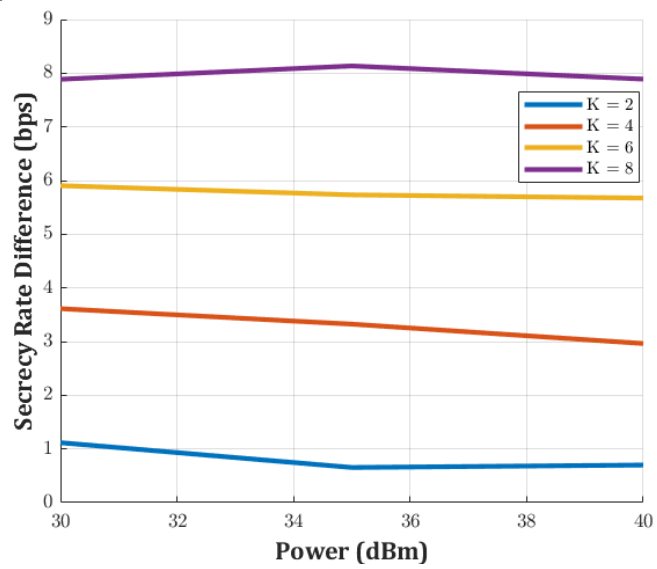


Figure 6. Impact of user density (K) on secrecy rate difference between BD-RIS and RIS

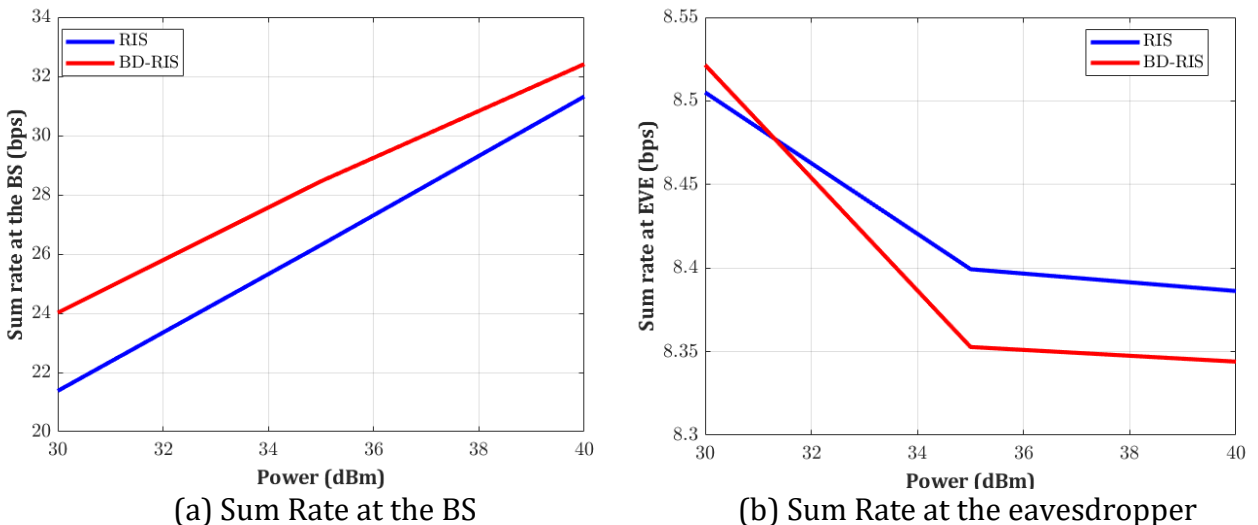


Figure 7. Sum rate comparison at the BS and the eavesdropper in RIS and BD-RIS systems.



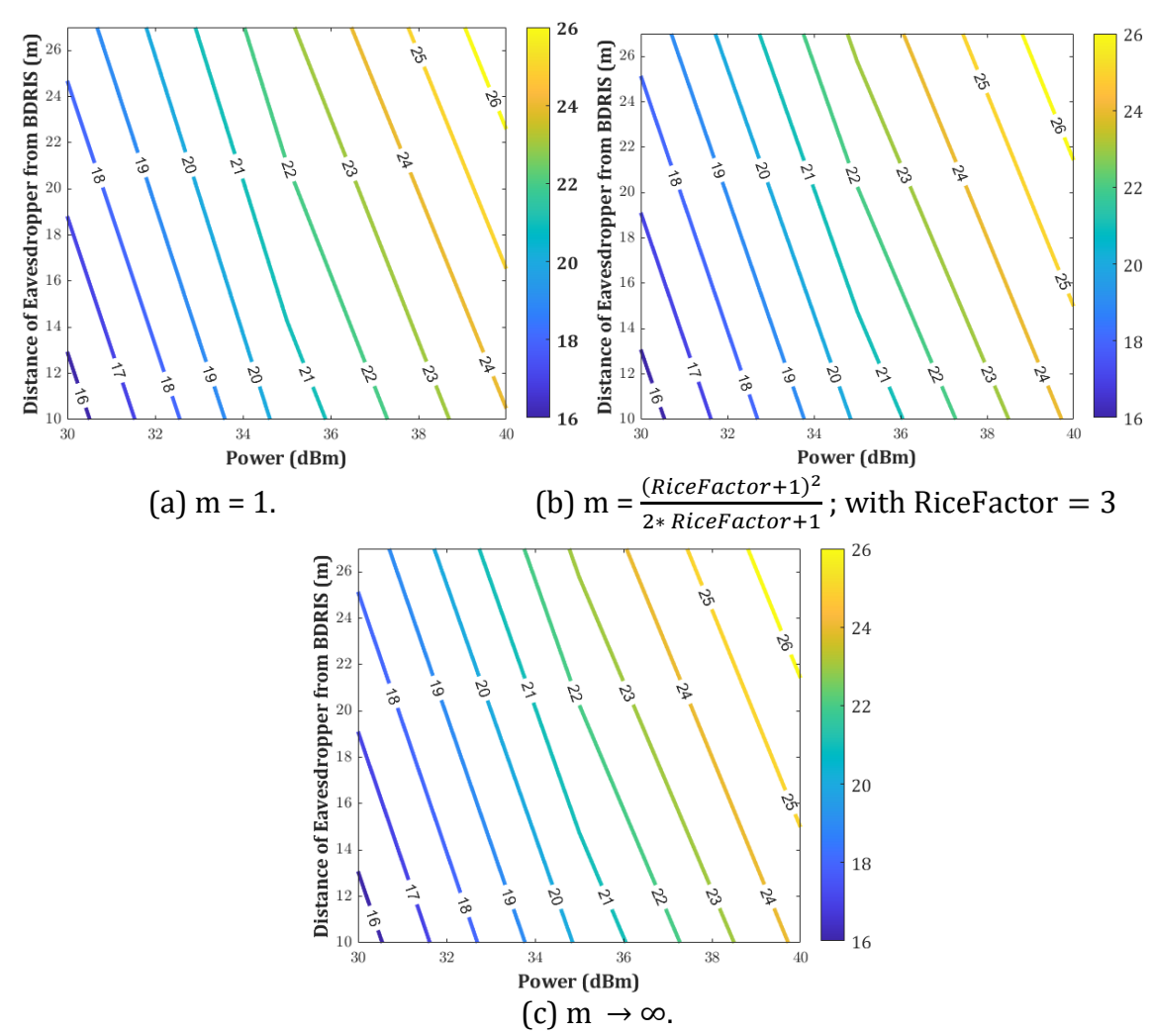


Figure 8. Effect of Nakagami-m channel parameter on the secrecy performance of a BD-RIS-assisted multi-user uplink system when direct link is blocked.

4. CONCLUSION

This work investigates a BD-RIS aided uplink multiuser MIMO communication system under Nakagami-m fading channel distribution in the presence of an eavesdropper. Through a detailed analysis, we demonstrated that BD-RIS significantly outperforms conventional diagonal RIS, with up to 8.33% improvement in secrecy rate in both scenarios (with and without direct transmission links). This enhancement is due to the non-diagonal scattering matrix architecture of BD-RIS, which enables a joint optimization of the magnitude and the phase of the impinging signal, thereby allowing more power allocation efficiency and directional beamforming. The simulation results further highlight that the secrecy rate of BD-RIS increase with higher transmit power, greater eavesdropper distance with respect to the BD-RIS position, and higher user density, stressing on its scalability for future dense wireless networks. While challenges such as implementation complexity and channel estimation remain open for future research, the findings of this study highlight the BD-RIS as a promising solution for robust physical layer security in next generation wireless communications.



NOMENCLATURE

Symbol	Description	Symbol	Description
M	Number of antennas at the BS	F	Channel matrix from BS to BD-RIS, size $M \times N$
N	Number of passive elements at the BD-RIS	R _{xx}	Transmit covariance matrix
K	Number of legitimate users	Ф	BD-RIS phase-shift matrix
d	Distance between transmitter and receiver (m)	Xi	Transmitted signal from i-th user
d_0	Reference distance (m)	y_{BS-i}	Received signal at the BS from i-th user
L(d)	Path loss at distance d (dB)	y_{EVE-i}	Received signal at the eavesdropper from i-th user
α	Path loss exponent	P _i	Transmit power of i-th user (dBm)
m	Nakagami-m fading parameter	σ^2	AWGN noise variance
Γ(·)	Gamma function	SINR	Signal-to-Interference-plus-Noise Ratio
Н	Channel matrix from BS to users, size $M \times K$	SR	Secrecy rate (bit/s/Hz)
G	Channel matrix from BD-RIS to users, size NxK		

Acknowledgements

This work was supported by the Department of Electronics and Communications Engineering, College of Engineering, University of Baghdad. The authors would also like to thank the Ministry of Higher Education and Scientific Research for its continued academic support.

Credit Authorship Contribution Statement

Mina Fadhil Hasan: Writing (original draft), Software, Methodology, Validation, Investigation. Aqiel Niama Almamori: Supervision, Conceptualization, Writing (review & editing), Validation.

Declaration of Competing Interest

The authors declare that they have no known competing financial interests or personal relationships that could have appeared to influence the work reported in this paper.

REFERENCES

Abdul Majed, M. and Omran, B., 2020. Pilot based channel estimation and synchronization in OFDM system. *Journal of Engineering*, 26(6), pp. 50–59. https://doi.org/10.31026/j.eng.2020.06.04.

Almamori, A. and Abbas, M.A., 2023. Channel state information estimation for reconfigurable intelligent surfaces based on received signal analysis. *International Journal of Electrical and Computer Engineering (IJECE)*, 13(2), pp. 1599–1605. https://doi.org/10.11591/ijece.v13i2.pp1599-1605.

Al-Nahhas, B., Obeed, M., Chaaban, A. and Hossain, M.J., 2021. RIS-aided cell-free massive MIMO: Performance analysis and competitiveness. In: 2021 IEEE International Conference on



Communications Workshops (ICC Workshops). pp. 1–6. https://doi.org/10.1109/ICCWorkshops50388.2021.9473521.

Basar, E., Renzo, M. Di, Rosny, J. De, Debbah, M., Alouini, M.S. and Zhang, R., 2019. Wireless communications through reconfigurable intelligent surfaces. *IEEE Access*, 7, pp. 116753–116773. https://doi.org/10.1109/ACCESS.2019.2935192.

Chen, J., Liang, Y.-C., Cheng, H. V and Yu, W., 2023. Channel estimation for reconfigurable intelligent surface aided multi-user mmWave MIMO systems. *IEEE Transactions on Wireless Communications*, 22(10), pp. 6853–6869. https://doi.org/10.1109/TWC.2023.3246264.

Demir, Ö.T. and Björnson, E., 2022. Is channel estimation necessary to select phase-shifts for RIS-assisted massive MIMO? *IEEE Transactions on Wireless Communications*, 21(11), pp. 9537–9552. https://doi.org/10.1109/TWC.2022.3177700.

Ding, F., 2023. Least squares parameter estimation and multi-innovation least squares methods for linear fitting problems from noisy data. *Journal of Computational and Applied Mathematics*, 426, P. 115107. https://doi.org/10.1016/j.cam.2023.115107.

Fang, T. and Mao, Y., 2024. A low-complexity beamforming design for beyond-diagonal RIS aided multi-user networks. *IEEE Communications Letters*, 28(1), pp. 203–207. https://doi.org/10.1109/LCOMM.2023.3333411.

Gao, B., Zhao, J., Yan, S. and Xiao, S., 2024a. Secrecy rate maximization for active reconfigurable intelligent surface assisted MIMO systems. *IEEE Access*, 12, pp. 87097–87109. https://doi.org/10.1109/ACCESS.2024.3416553.

Gao, N., Yao, Y., Jin, S., Li, C. and Matthaiou, M., 2024b. RIS-assisted simultaneous transmission and secret key generation: An ICAS paradigm. In: *IEEE INFOCOM 2024 - IEEE Conference on Computer Communications Workshops (INFOCOM WKSHPS)*. pp. 1–6. https://doi.org/10.1109/INFOCOMWKSHPS61880.2024.10620776.

Gómez-Déniz, E. and Gómez-Déniz, L., 2024. A new derivation of the Nakagami-m distribution as a composite of the Rayleigh distribution. *Wireless Networks*, 30(5), pp. 3051–3060. https://doi.org/10.1007/s11276-024-03713-5.

Hamza, K.M., Basharat, S., Jung, H., Gidlund, M. and Hassan, S.A., 2024. Secrecy analysis of RIS-assisted uplink NOMA systems under Nakagami-m fading. In: *2024 IEEE International Conference on Communications Workshops (ICC Workshops)*. pp. 1511–1516. https://doi.org/10.1109/ICCWorkshops59551.2024.10615519.

Ji, Z., Yeoh, P.L., Zhang, D., Chen, G., Zhang, Y., He, Z., Yin, H. and li, Y., 2021. Secret key generation for intelligent reflecting surface assisted wireless communication networks. *IEEE Transactions on Vehicular Technology*, 70(1), pp. 1030–1034. https://doi.org/10.1109/TVT.2020.3045728.

Karim, D., Al-Hindawi, A. and Shather, A., 2023. Modeling and simulating NOMA performance for next generations. *Journal of Engineering*, 29(04), pp. 155–175. https://doi.org/10.31026/j.eng.2023.04.11.

Khaled, Z. El, Ajib, W. and Mcheick, H., 2022. Log distance path loss model: application and improvement for sub 5Ghz rural fixed wireless networks. *IEEE Access*, 10, pp. 52020–52029. https://doi.org/10.1109/ACCESS.2022.3166895.

Khoshafa, M.H., Maraqa, O., Moualeu, J.M., Aboagye, S., Ngatched, T.M.N., Ahmed, M.H., Gadallah, Y. and Renzo, M.D., 2024. RIS-assisted physical layer security in emerging RF and optical wireless



communication systems: A comprehensive survey. *IEEE Communications Surveys & Tutorials*, P. 1. https://doi.org/10.1109/COMST.2024.3487112.

Laas, T., Nossek, J.A., Bazzi, S. and Xu, W., 2020. On reciprocity in physically consistent TDD systems with coupled antennas. *IEEE Transactions on Wireless Communications*, 19(10), pp. 6440–6453. https://doi.org/10.1109/TWC.2020.3003414.

Li, H., Shen, S. and Clerckx, B., 2023a. Beyond diagonal reconfigurable intelligent surfaces: A multisector mode enabling highly directional full-space wireless coverage. *IEEE Journal on Selected Areas in Communications*, 41(8), pp. 2446–2460. https://doi.org/10.1109/JSAC.2023.3288251.

Li, H., Shen, S. and Clerckx, B., 2023b. Beyond diagonal reconfigurable intelligent surfaces: from transmitting and reflecting modes to single-, group-, and fully-connected architectures. *IEEE Transactions on Wireless Communications*, 22(4), pp. 2311–2324. https://doi.org/10.1109/TWC.2022.3210706.

Li, H., Shen, S., Nerini, M. and Clerckx, B., 2024a. Reconfigurable intelligent surfaces 2.0: Beyond diagonal phase shift matrices. *IEEE Communications Magazine*, 62(3), pp. 102–108. https://doi.org/10.1109/MCOM.001.2300019.

Li, H., Shen, S., Nerini, M., Renzo, M. Di and Clerckx, B., 2024b. Beyond diagonal reconfigurable intelligent surfaces with mutual coupling: Modeling and optimization. *IEEE Communications Letters*, 28(4), pp. 937–941. https://doi.org/10.1109/LCOMM.2024.3361648.

Li, H., Shen, S., Zhang, Y. and Clerckx, B., 2024c. Channel estimation and beamforming for beyond diagonal reconfigurable intelligent surfaces. *IEEE Transactions on Signal Processing*, 72, pp. 3318–3332. https://doi.org/10.1109/TSP.2024.3424229.

Liu, Y., Mu, X., Xu, J., Schober, R., Hao, Y., Poor, H. V and Hanzo, L., 2021. Star: Simultaneous transmission and reflection for 360° coverage by intelligent surfaces. *IEEE Wireless Communications*, 28(6), pp. 102–109. https://doi.org/10.1109/MWC.001.2100191.

Mishra, A., Mao, Y., D'Andrea, C., Buzzi, S. and Clerckx, B., 2024. Transmitter side beyond-diagonal reconfigurable intelligent surface for massive MIMO networks. *IEEE Wireless Communications Letters*, 13(2), pp. 352–356. https://doi.org/10.1109/LWC.2023.3329065.

Mohammed, S. and Almamori, A., 2024. Cell-free massive MIMO energy efficiency improvement by access points iterative selection. *Journal of Engineering*, 30(03), pp. 129–142. https://doi.org/10.31026/j.eng.2024.03.09.

Mohammed, S.A., 2020. Securing physical layer for FHSS communication system using code and phase hopping techniques in CDMA, system design and implementation. *Journal of Engineering*, 26(7), pp. 190–205. https://doi.org/10.31026/j.eng.2020.07.13.

Nerini, M., Shen, S. and Clerckx, B., 2024. Closed-form global optimization of beyond diagonal reconfigurable intelligent surfaces. *IEEE Transactions on Wireless Communications*, 23(2), pp. 1037–1051. https://doi.org/10.1109/TWC.2023.3285262.

Nerini, M., Shen, S., Li, H. and Clerckx, B., 2024. Beyond diagonal reconfigurable intelligent surfaces utilizing graph theory: Modeling, architecture design, and optimization. *IEEE Transactions on Wireless Communications*, 23(8), pp. 9972–9985. https://doi.org/10.1109/TWC.2024.3367631.

Samy, M., Al-Hraishawi, H., Adam, A.B.M., Chatzinotas, S. and Otteresten, B., 2025. Beyond diagonal RIS-aided networks: Performance analysis and sectorization tradeoff. *IEEE Open Journal of the Communications Society*, 6, pp. 302–315. https://doi.org/10.1109/OJCOMS.2024.3514696.



Santamaria, I., Soleymani, M., Jorswieck, E. and Gutiérrez, J., 2024. Mimo capacity maximization with beyond-diagonal RIS. In: *2024 IEEE 25th International Workshop on Signal Processing Advances in Wireless Communications (SPAWC)*. pp. 936–940. https://doi.org/10.1109/SPAWC60668.2024.10694491.

Shen, S., Clerckx, B. and Murch, R., 2022. Modeling and architecture design of reconfigurable intelligent surfaces using scattering parameter network analysis. *IEEE Transactions on Wireless Communications*, 21(2), pp. 1229–1243. https://doi.org/10.1109/TWC.2021.3103256.

Singh, S., Raviteja, A., Singh, K., Singh, S.K., Kaushik, A. and Ku, M.L., 2024. Secrecy rate maximization for active RIS-aided robust uplink NOMA communications. *IEEE Wireless Communications Letters*. https://doi.org/10.1109/LWC.2024.3424332.

Tang, W., Chen, X., Chen, M.Z., Dai, J.Y., Han, Y., Jin, S., Cheng, Q., Li, G.Y. and Cui, T.J., 2021. On channel reciprocity in reconfigurable intelligent surface assisted wireless networks. *IEEE Wireless Communications*, 28(6), pp. 94–101. https://doi.org/10.1109/MWC.001.2100136.

Wu, C., You, C., Liu, Y., Gu, X. and Cai, Y., 2022. Channel estimation for star-RIS-aided wireless communication. *IEEE Communications Letters*, 26(3), pp. 652–656. https://doi.org/10.1109/LCOMM.2021.3139198.

Yahya, H., Li, H., Nerini, M., Clerckx, B. and Debbah, M., 2024. Beyond diagonal RIS: Passive maximum ratio transmission and interference nulling enabler. *IEEE Open Journal of the Communications Society*, 5, pp. 7613–7627. https://doi.org/10.1109/OJCOMS.2024.3509220.

Yang, S., Han, H., Liu, Y., Guo, W., Pang, Z. and Zhang, L., 2023. Reconfigurable intelligent surface-induced randomness for mmWave key generation. In: *ICC 2023 - IEEE International Conference on Communications*. pp. 2909–2914. https://doi.org/10.1109/ICC45041.2023.10278950.

Zhang, H., Ma, S., Shi, Z., Zhao, X. and Yang, G., 2023. Sum-rate maximization of RIS-aided multi-user MIMO systems with statistical CSI. *IEEE Transactions on Wireless Communications*, 22(7), pp. 4788–4801. https://doi.org/10.1109/TWC.2022.3228910.

Zhou, G., Peng, Z., Pan, C. and Schober, R., 2024. Individual channel estimation for RIS-aided communication systems—A general framework. *IEEE Transactions on Wireless Communications*, 23(9), pp. 12038–12053. https://doi.org/10.1109/TWC.2024.3387563.



تعزيز أمان الطبقة المادية من خلال BD-RIS: تحليل مقارن لمعدل السرية في شبكات Mimo متعددة المستخدمين مع تلاشي

مينا فاضل حسن *، عقيل نعمة المعموري

قسم هندسة الإلكترونيك والاتصالات، كلية الهندسة، جامعة بغداد، بغداد، العراق

الخلاصة

مع نقدم الشبكات اللاسلكية نحو الجيل السادس، لا يزال الأمن يُشكل مصدر قلق بالغ نظرًا لطبيعة البث المتأصلة فيها، مما يجعلها عرضة للتنصت والاعتراض غير المصرح به. تُعزز تقنية الأسطح الذكية القابلة لإعادة التكوين (BD-RIS) التحكم في القنوات اللاسلكية من خلال التحكم بشكل مستقل في طور وحجم الإشارات المنعكسة، مما يُحسّن أمان الطبقة المادية لأنظمة BD- الاتصالات اللاسلكية. تبحث هذه الورقة البحثية في أداء نظام MIMO متعدد المستخدمين للوصلة الصاعدة بمساعدة -RIS والذي يعمل في ظل ظروف تلاشي Nakagami-m بوجود منصت سلبي. وبشكل أكثر تحديدًا، نُحلل ونقارن معدل المجموع المُمكن تحقيقه ومعدل السرية في سيناريوهات، سواءً بوجود رابط مباشر بين المستخدمين ومحطة القاعدة أو بدونه. من خلال عمليات محاكاة مُفصلة، نُظهر أن تقنية BD-RIS تُعزز بشكل كبير معدل السرية مُقارنةً بتقنية RIS القطرية التقليدية، مُحققةً تحسنًا بنسبة 83.38%. وعلاوة على ذلك، نُظهِر أن حجم هذا التعزيز يتأثر بمعلمات النظام الرئيسية، بما في ذلك قوة الإرسال، ومسافة المتنصت، وكثافة المستخدمين النشطين داخل الشبكة.

الكلمات المفتاحية: BD-RIS، معدل السرية، MIMO متعدد المستخدمين، تلاشي Nakagami-m، أمان الطبقة المادية (PLS).